Lab on a Chip

RSC Publishing

PAPER

View Article Online
View Journal | View Issue

Cite this: *Lab Chip*, 2013, **13**, 4848

New perspectives for direct PDMS microfabrication using a CD-DVD laser†

M. Hautefeuille,*[a] L. Cabriales,[a] R. Pimentel-Domínguez,[a] V. Velázquez,[a] J. Hernández-Cordero,[b] L. Oropeza-Ramos,[c] M. Rivera,[d] M. P. Carreón-Castro,[e] M. Grether[a] and E. López-Moreno[a]

Received 12th September 2013,
Accepted 27th September 2013

DOI: 10.1039/c3lc51041g

www.rsc.org/loc

A simple and inexpensive alternative to high-power lasers for the direct fabrication of microchannels and rapid prototyping of poly-dimethylsiloxane (PDMS) is presented. By focusing the infrared laser beam of a commercial, low-power CD-DVD unit on absorbing carbon micro-cluster additives, highly localized PDMS combustion can be used to etch the polymer, which is otherwise transparent at such wavelengths. Thanks to a precise and automated control of laser conditions, laser-induced incandescence is originated at the material surface and produces high-resolution micropatterns that present properties normally induced with lasers of much greater energies in PDMS: formation of *in situ* nanodomains, local fluorescence and waveguide patterns. An extensive study of the phenomenon and its performance for PDMS microfabrication are presented.

Introduction

The interesting electrical, mechanical and optical properties of poly(dimethylsiloxane) (PDMS) have motivated a widespread utilization of this low-cost and accessible material in tridimensional microstructures with countless applications, including microfluidics and photonics.[1–3] The biocompatibility of PDMS is further widening its range of applications to biomedical research fields for developing polymer-based biosensors and tissue engineering platforms.[4–6] In order to produce micron-range cast-moulding PDMS stamps with the desired tridimensional features, photolithographic techniques are generally required in order to construct the initial moulds onto which the liquid polymer is cast and cross-linked. This process then provides a PDMS replica of the structures of the mould with great fidelity. Although photolithographic moulds offer excellent resolution, the fabrication process is relatively expensive or complicated for some applications where rapid prototyping is needed. The main advantage of PDMS, besides its unique combination of intrinsic properties and affordable cost, is the series of straightforward soft lithography techniques that may be readily used for micropatterning elastomeric layers on demand, circumventing the need for traditional but expensive processes.[7,8]

In some applications where PDMS layers require further selective functionalization or self-assembly patterning, localized chemical or physical surface modification techniques may also be employed.[4,9] For instance, improved bonding to other substrates or coatings is possible by exposing the PDMS surface to ultraviolet (UV) light,[10] O_2 plasma,[11] corona discharge[12] or different chemical and thermal treatments.[13] Although these procedures have been demonstrated to be effective for PDMS rapid prototyping, the resulting modified surfaces may be relatively delicate to manipulate and in many cases the effect is very limited in time.[14]

Recently, simpler and more direct microfabrication processes are using lasers to etch superficial patterns or tridimensional structures in a large variety of materials. High-resolution moulds can be readily fabricated with lasers to allow the subsequent use of the PDMS replica-mould technique in a two-step fashion.[15,16] High-energy, short-pulsed lasers are also used for direct micromachining of PDMS layers in a single step,[17,18] or to create fine features like capillaries in soft-lithographic PDMS moulds.[19] Uncured liquid PDMS may also be locally cross-linked using femtosecond (fs) laser pulses, due to the volume-constrained temperature rise

[a] *Facultad de Ciencias, Universidad Nacional Autónoma de México, Avenida Universidad 3000, Circuito Exterior S/N, Ciudad Universitaria, Delegación Coyoacán, C.P. 04510, D. F. México, México. E-mail: mathieu_h@ciencias.unam.mx*
[b] *Instituto de Investigaciones en Materiales, Universidad Nacional Autónoma de México, Avenida Universidad 3000, Circuito Exterior S/N, Ciudad Universitaria, Delegación Coyoacán, C.P. 04510, D. F. México, México*
[c] *Facultad de Ingeniería, Universidad Nacional Autónoma de México, Avenida Universidad 3000, Circuito Exterior S/N, Ciudad Universitaria, Delegación Coyoacán, C.P. 04510, D. F. México, México*
[d] *Instituto de Física, Universidad Nacional Autónoma de México, Avenida Universidad 3000, Circuito Exterior S/N, Ciudad Universitaria, Delegación Coyoacán, C.P. 04510, D. F. México, México*
[e] *Instituto de Ciencias Nucleares, Universidad Nacional Autónoma de México, Avenida Universidad 3000, Circuito Exterior S/N, Ciudad Universitaria, Delegación Coyoacán, C.P. 04510, D. F. México, México*

† Electronic supplementary information: An example of a simple square pattern etched by a low-power laser at low resolution (slow stage displacement) is presented in the supplemental video. See DOI: 10.1039/c3lc51041g

that polymerizes the material selectively and locally.[20] Depending on the desired applications, high power lasers are also used to generate local physical or chemical transformations of the PDMS surface to create micro-arrays of integrated photonics elements[17] or highly hydrophobic microfluidic channels for all-polymer and heterogeneous devices.[21] High-energy ultraviolet lasers are also employed to promote the adhesion of metallic layers in etched channels for further fabrication of synthetic nerves for medical applications.[22] In general, the lasers used for these processes are expensive, thus limiting the widespread use of this technique for rapid prototyping.

In this work, we demonstrate the use of a low-cost optical setup based on a modern CD-DVD pickup head (PUH) for direct PDMS micropatterning. The proposed arrangement provides two laser diodes mounted on a three-axis platform with computer-controlled micrometer-range displacements for direct PDMS micropatterning.[23] Typically, the low absorption of visible or NIR light by PDMS impedes the use of these wavelengths for direct etching with such low-power lasers. However, the addition of carbon nanoparticles (CNP) absorbing the two wavelengths available from the PUH (650 nm and 785 nm) can generate localized laser-induced incandescence when excited by a focused laser beam, as observed for carbon nanotubes in a vacuum.[24,25] Indeed, when the laser is shone onto the additive-modified polymeric material it causes a very rapid and localized temperature rise that can be controlled, sustained for a long time or used for precise and local PDMS etching.[26] By taking advantage of this phenomenon, the PUH allows the simple and direct fabrication of micron-range structures in CNP-modified PDMS. An extensive study of this nanoparticle-enhanced laser etching method is presented in this paper.

Experiment and samples preparation

Optical setup

The laser setup used in this work is based on the optical pickup head (PUH) of a commercial CD-DVD system from a *Super Multi Lightscribe* CD-DVD burner mounted on a three-axis micro-displacement stage with computer numerical control (CNC) (Fig. 1).[23] Although the platform offers two wavelengths, only the near-infrared (NIR) laser diode (785 nm) has been used in this work, as it presented better laser-induced incandescence results. A laser beam with controllable power densities of up to 80 mW cm^{-2}, in either continuous or pulsed mode, can be focused onto the sample surface with a diameter of only one micrometre. As the PDMS samples used in this work are translucent, a charge coupled device (CCD) camera coupled to a 20× magnification microscope objective allowed for visualizing and correcting the laser alignment, sample displacement and ablation procedure in real time. For this purpose, a bright light emitting diode was attached near the focal lens of the PUH to illuminate the sample. Finally, a small telescope with an additional CCD camera was mounted with a set of lenses at the side of the sample to observe the incandescence phenomenon.

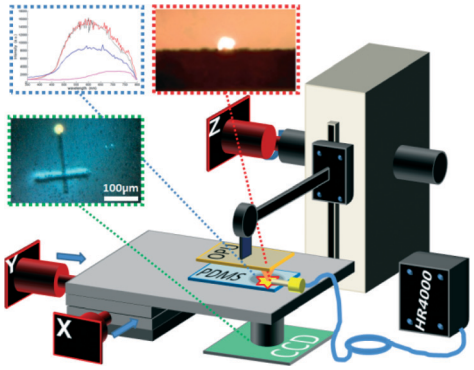

Fig. 1 Diagram of the low-cost laser setup used to characterize laser-induced incandescence in additive-modified PDMS.

Alternatively, the camera and the lenses were replaced by an optical fibre placed in close proximity to the sample and connected to a spectrophotometer (Ocean Optics HR4000) in order to characterize the incandescence spectra (see Fig. 1).

Materials and samples preparation

Carbon nanoparticles were spread onto or embedded into PDMS layers (Sylgard 184 from Dow Corning) in low concentrations. The carbon-based materials were purchased from Sigma Aldrich (carbon nanopowder, part no. 633 100, multi-walled carbon nanotubes, part no. 724 769) and used without further treatment.

For characterization purposes, two different sets of PDMS samples with additives were prepared. In the first set of samples, a small amount of carbon additive was cast and spread homogeneously over the surface of clean, cross-linked PDMS layers using a Doctor Blade casting technique. In the second set of samples, the additive materials were incorporated in concentrations below 5% in weight inside the liquid elastomer to create composites. To achieve a homogeneous distribution of the dry materials within the PDMS host matrix, a 10 min sonication was performed before polymer cross-linking. In both cases (cast or embedded layers), polymeric samples were prepared with a standard procedure by mixing PDMS pre-polymer with curing agent in a 10 : 1 weight-ratio. Final curing of the samples was performed by heating in a convective oven at 80 °C for at least 2 h. Layers with thicknesses ranging from 100 μm to a few millimetres were produced with this method.

Characterization of laser-induced incandescence for PDMS etching

High-power laser processing of PDMS has been shown to provide features such as wettability modification,[27] fluorescence,[28] non-reciprocal ablation as a function of laser etching direction[29] and local formation of polymer-derived nanodomains as by-products of the combustion.[30] As shown in the following sections, similar effects can be observed using the low-cost PUH.

Conditions for the generation of laser-induced incandescence

The laser in the PUH generates a highly localized photothermal effect in the carbon nanopowder filling or spread onto the PDMS layers. This leads to laser-induced incandescence, which manifests itself as a bright visible emission and is obtained under ambient conditions of temperature, humidity and pressure (typically 20 °C, 35% of relative humidity and 0.76 atm in our laboratory) when the laser is precisely focused on the additive material clusters above a certain power density threshold.

Incandescence in the PDMS layers can be induced under ambient conditions provided that the additive particles fulfil two important conditions. First, it is necessary to guarantee low percolation and micron-size clustering of the additive materials. A very rapid and highly localized temperature increase, leading to PDMS micro-etching, seems to be guaranteed only when the additive clusters and the spot-size of the IR laser have comparable dimensions. Also, additive concentration plays an important role as greater densities may limit or impede combustion, probably due to enhanced thermal transport into the PDMS host layer in a heat sink fashion, thus decreasing the local rise in temperature. However, low percolation conditions seem to limit conductive thermal transport from the small additive clusters under illumination through the medium, as PDMS acts as an excellent thermal barrier (a typical thermal conductivity of $\kappa \sim 0.16$ W m^{-1} K^{-1} is reported).[31]

The second condition for incandescence is that the clusters are motion-constrained. It has been observed that when the clusters are free to move on the surface, the heat generated by laser light absorption is sufficient to instantly expel them away from the focal point. This laser-induced nanoparticle propulsion has been previously reported using femtosecond lasers.[32] In elastic PDMS layers, the section of the PDMS host membrane illuminated by NIR laser light may be deformed,[33] forcing the refocusing of the laser to optimize the incandescence conditions. Nonetheless, the surfaces of cured-PDMS pristine layers allow for the additive materials to adhere to the surface and are thus adequate for PDMS etching with laser-induced incandescence.

Characterization of emission spectra

The spectra of visible emissions registered during incandescence show a bell-shaped profile centred in the visible region (Fig. 2). In contrast, light emission from carbon based particles has been shown to present a wide infrared tail characteristic of blackbody radiation behaviour.[24,25] A red shift in the central wavelength of the spectrum was also observed when additives were incorporated into the PDMS layers.

Some narrow peaks have also appeared occasionally at constant wavelengths during measurements. This phenomenon seems likely to be caused by the generation of local micro-plasma, as seen in Laser-Induced Breakdown Spectroscopy (LIBS).[34] The roughness caused by the presence of microclusters is indeed an important factor in the generation of plasma, as it may be responsible for localized intense electric field enhancements. In this case, the emission in PDMS would then be related to matter ionization, and these occasional peaks might provide information about the nature of the underlying PDMS. Spectral analysis confirmed this hypothesis, as the location of the peaks demonstrate the presence of the three main elements of PDMS: carbon (in the $2s^2 2p3p$ form at 581.4 nm and 656.9 nm), silicon ($3s3p^2 3s^2 4p$ at 390.6 nm) and oxygen ($2s^2 2p^3(2D^0)3s$ at 382.3 nm).[35]

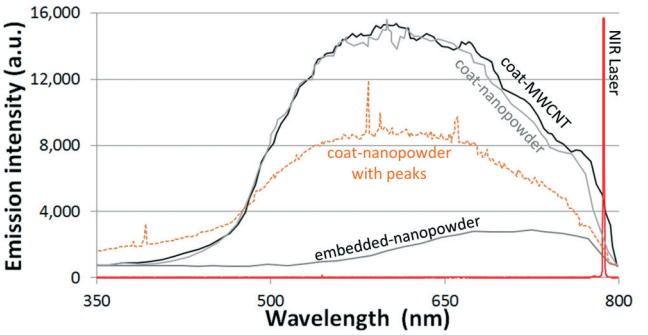

Fig. 2 Spectra of laser-induced incandescence in PDMS for different additive materials and sample types when excited with a 785 nm laser at 65 mW cm^{-2} (5 ms pulse).

Characterization of emission intensity

The duration and intensity of laser-induced incandescence were also measured. As will be shown in the following sections, these parameters play a significant role in the etching resolution and the physicochemical properties of the processed samples. The duration of short emissions caused by laser pulses was monitored with an optical fibre located at the PDMS surface and a photomultiplier tube with an IR optical filter. In most cases, the emission decay time was found to be in the order of a few hundreds of microseconds, similar to those previously reported under similar experimental conditions.[36]

In general, the emission lifetime and intensity were found to be much greater for coatings than for fillers, all other parameters remaining equal. Sustained emission was also characterized using CW laser exposure. In this case, the intensity depends directly on the power density of the laser (Fig. 3a). As seen in the figure, the emission intensity as a function of excitation power density can be fit to an asymptotic function with a characteristic power density of 29 mW cm^{-2}. When laser excitation was maintained for a long time, a sustained visible emission was also observed in the samples with cast additives, lasting for as long as 30 minutes.

The intensity decay time of the sustained emission was also measured. As seen in Fig. 3b, the experimental data fit an exponential decay with a characteristic decay time (τ_{decay}) ranging from 90 s to 120 s. These decay times are shorter than those calculated from other experiments involving PDMS combustion. Nonetheless, they are within the same order of magnitude. Remarkably, this characteristic exponential decay is similar to the heat release rate measured in the PDMS pyrolysis process.[38]

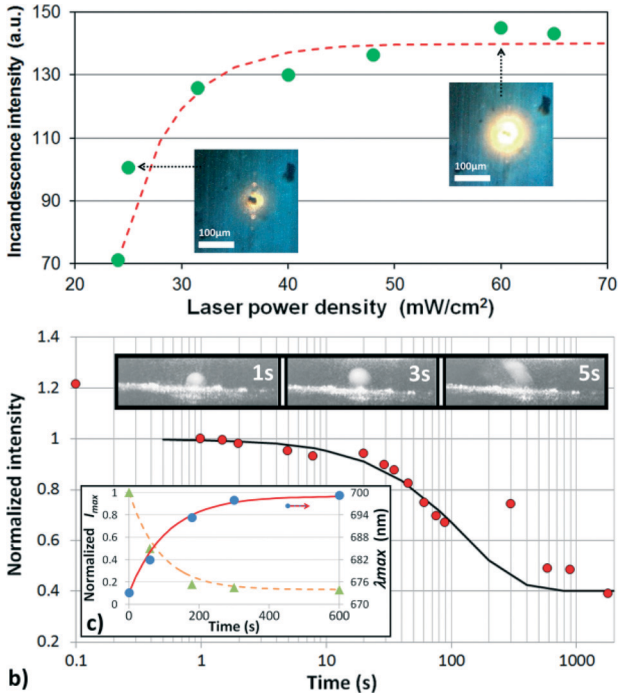

Fig. 3 Intensity of the sustained incandescence of PDMS coated with carbon nanopowder as a function of (a) laser power density and excitation time at 65 mW cm^{-2} obtained (b) from the visualization CCD and (c) from the spectrophotometer. Dots are experimental values and lines are fitted models.

Further information of the spectral and intensity evolution of the PDMS emission is shown in Fig. 3c. The emission spectrum is rapidly shifted towards longer wavelengths, confirming previous observations of laser-induced emission in carbon nanomaterials.[24,25] This shift in wavelength also presents an asymptotic exponential behaviour that fits the experimental data, with a characteristic shift time (τ_{shift}) of 110 s, similar to the intensity decay time.

Characterization of etched PDMS physicochemical properties

A high temperature rise due to optical absorption by the particles leads to incandescence of the PDMS layers. It has been shown that local temperatures of 1000 K–1750 K may be reached in carbon nanoparticle clusters with NIR laser power densities no greater than 2 W cm^{-2}.[24,25,31] Since PDMS combustion normally takes place at such temperatures,[39] this photothermal effect could be used for etching PDMS layers.

PDMS direct laser microetching

A small amount of fumes are evident when incandescence occurs, and a small superficial volume of PDMS is removed after the phenomenon has taken place. Thanks to the CNC capabilities of the laser platform, channel-like micropatterns have been successfully etched in the PDMS layers. For PDMS layers with casting additives, the resolution of the etched microchannels depends on the laser power density and dwell time (see ESI†). Optimal resolution has been obtained in the CW mode at the greatest displacement velocities (*i.e.*, shortest dwell time). In this case, it was possible to etch features with a maximum lateral resolution of approximately 10 µm where the spot is hitting the surface. As demonstrated in previous work, NIR light absorption by embedded additive particles may also cause a PDMS deformation as a collateral effect.[33] This deformation is also proportional to laser power density. Despite the low thermal conductivity of PDMS, the laser beam is indeed highly focused on the surface and a small peripheral region around the focal spot is thus slightly deformed during the process, especially in the CW mode. In this case the thermal out-of-plane expansion is noticeable with the visualization CCD unit. For practical purposes, this defocusing may cause a resolution loss of up to 30% in the worst case. By contrast, this side-effect does not occur in the coated PDMS layers. The photo-induced deformation can be limited by sandwiching the layers between two glass slides during fabrication. These did not impede laser direct etching and even increased the resolution by 30% on average, proving that out-of-plane expansion was indeed responsible for the loss of resolution.

Residual materials

For all types of samples, visible residues were always found in the PDMS laser etched channels. While a thin white powder appeared at low power densities, a black (shiny or dark) powder was obtained when the layers were processed at higher laser powers. These residues were easily removed from the channels simply by cleaning the surface with an aqueous solvent and rinsing with water. Incandescence may be induced again by focusing the IR laser on these residues inside the existing etched channels or wells, even months after the initial etching, if they are not removed. This is most likely due to the nature of the residual micro or nanoscale material left as an ablation by-product, which will play the role of a new absorbing additive capable of triggering laser incandescence again.

The residual products were analysed by a scanning electron microscope (SEM, *Jeol JSM5600 LV*) coupled to a *NORAN* energy dispersive spectrophotometer (EDS) working at 20 keV. Fourier-Transform infrared spectroscopy with attenuated total reflectance (ATR-FTIR, *Perkin Elmer FTIR Spectrum 100*) and Raman spectroscopy (*Thermo Scientific DXR Raman microscope*) were also employed in this analysis.

Typical images of the residual materials observed with polarized microscopy are shown in Fig. 4b. The ATR-FTIR spectra for both pristine and etched PDMS samples are presented in Fig. 5. Although a shift in the position of the absorbance maximum is observed in the spectra (792 cm^{-1} and 1015 cm^{-1}), both are too similar to demonstrate chemical modifications caused by laser processing, as previously shown for PDMS.[37] A low hydroxyl group absorbance band is also registered between 3200 cm^{-1} and 3400 cm^{-1} in the etched PDMS channels.

The different colours observed by polarized-light microscopy seem to indicate that some oriented micro and

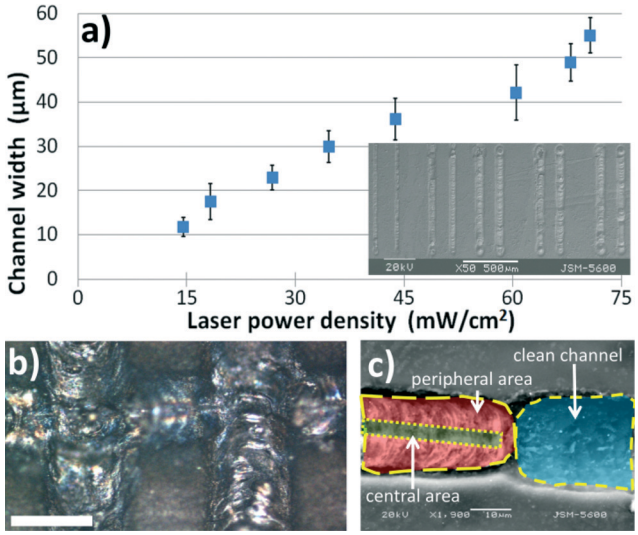

Fig. 4 Dimensions of etched channels as a function of laser power density (a). Micrograph of crossing channels etched at 65 mW cm^{-2} (scale bar is 20 µm) (b); and SEM micrograph of a channel etched at 65 mW cm^{-2} for EDS analysis (c).

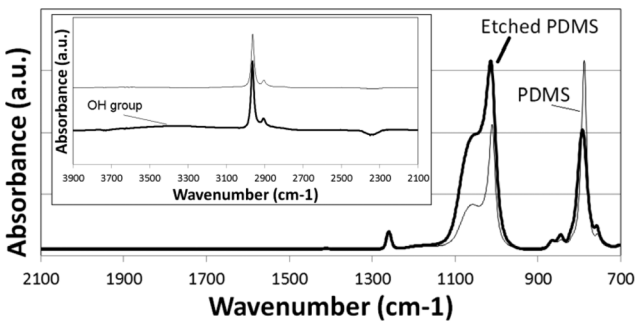

Fig. 5 ATR-FTIR normalized spectra of virgin and residual material of channels etched in PDMS at 65 mW cm^{-2}

nanodomains are present in the central and peripheral regions of etched volumes (Fig. 4b). A more localized analysis of the residues was performed using an EDS. Different textures are visible in SEM micrographs, in particular, in the central regions of the spot where the laser is more intense. Table 1 summarizes the results obtained for different samples and at different regions and different laser power densities. Clearly, the composition of the residues depends strongly on the region (and thus on laser intensity); noticeably, carbon is present in the regions where the temperature was higher during the etching process, *i.e.*, at the laser focal point. This agrees with previous studies on PDMS combustion by-products, where different residues are observed at different temperatures.[39] Typically, SiO_2 is obtained at the lowest temperatures of the combustion process and silicon oxycarbide or silicon carbide may be formed as the processing temperature increases.

To further study these residues, a Raman scattering spectroscopy characterization was performed. The G band (1580 cm^{-1}) and D band (1345 cm^{-1}), characteristic of graphitic carbon nanodomains, are clearly present inside the etched PDMS patterns (Fig. 6). The laser-induced incandescence process thus generates localized thermal formation of carbon nanocrystals without the need for high-power irradiation.[40] Even after washing the ablated patterns, the nanodomains are still visible. They are probably embedded under the surface, as reported in ref. 41. However, unlike other works with high-power lasers in PDMS, no SiC or SiCO semiconducting structures have been observed. This may be explained by the thermal conditions for PDMS ablation, since factors such as heating rate, temperature during laser exposure and even nanoparticle additives greatly influence the nature of the by-products.[36,38,42]

Hydrophobicity increase

High-power laser surface treatment increases PDMS hydrophobicity, mainly because of micro or nanopattern formation at the surface of the polymer.[39] In ref. 27, a CO_2 laser was used to vulcanize PDMS and modify its roughness and wettability with pulses of 5 J cm^{-2}. The etched microstructures with nanostructured residual materials obtained in PDMS

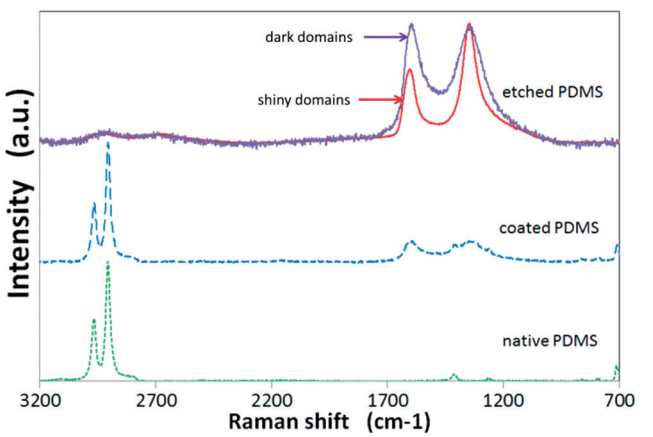

Fig. 6 Raman spectra of pristine, coated and etched PDMS. Dark and shiny domains were obtained from two different laser power densities.

Table 1 Elemental weight composition, measured by SEM-EDS, of pristine PDMS and combustion residual material found inside the channels

		Element weight (%) of residual material in laser etched PDMS layers			
Element	Element weight (%) in pristine PDMS	Central region 65 mW cm^{-2}	Peripheral region 65 mW cm^{-2}	Peripheral region 45 mW cm^{-2}	Peripheral region 30 mW cm^{-2}
O	38.68	29.28	52.07	49.07	46.26
Si	30.56	47.54	47.93	50.93	53.74
C	30.77	23.18	Traces	Traces	Traces

here then suggest that the low-power laser-induced incandescence may allow for the generation of local surface modification to enhance the hydrophobicity of selected PDMS areas. This phenomenon is especially interesting for its potential use in microfluidic and biomedical applications with the generation of a super hydrophobic, self-cleaning material surface. The impact of sidewall roughness on the microfluidic performance of the resulting channels has yet to be addressed. However, the laser parameters (*e.g.*, power and dwell time) as well as proper cleaning of the resulting trenches seem to play an important role in determining the average roughness.

Water contact angles (CA) have been measured for 3 mm by 3 mm areas of virgin and laser-etched PDMS with a Pocket Goniometer (PG-3 model). Clean virgin surfaces presented a typical CA of 106.1° ± 2.3° whereas all etched PDMS surfaces presented a greater CA of 129.6° ± 3.1°. These results demonstrate that the present technique can be employed to induce a local hydrophobicity increase of PDMS surfaces, and thus offers a much simpler solution than existing ones where chemicals or high-power lasers must be employed.

It has also been observed that this laser surface modification was not a function of laser intensity and was persistent. Interestingly, the process does not impede further treatment by corona discharge to form a temporal hydrophilic PDMS surface with a CA lower than 20°. In this case, the surface recovers its highly hydrophobic state in a few hours. This supports the idea that roughness modification is responsible for the hydrophobicity increase, as opposed to a chemical transformation being involved in this process.

Microphotonics applications

All the obtained etched micropatterns presented local fluorescence in the visible range when illuminated under ultraviolet light. This consequence of PDMS laser ablation is already known, and has potential applications in opto-microfluidics.[18,28] Fluorescence was characterized with an inverted fluorescence microscope (*Nikon Diaphot*) equipped with a *SensSys* CCD camera and a green visualization filter. Interestingly, the average intensity was dependent on the laser power density used to etch PDMS (see Fig. 7). A characteristic power density of 33.5 mW cm^{-2} was calculated from the exponential fit of the experimental curve. It is comparable to the characteristic power density of 31 mW cm^{-2} fitting the incandescence emission intensity of Fig. 3a. It is also important to remark that fluorescence was more intense in areas free of residues. This confirms the results from the micro-Raman characterization indicating that carbon nanocrystals seem to be embedded in clean etched volumes, as reported in ref. 41.

Channels etched in 3 mm-thick PDMS samples at the highest power density have also been tested as waveguides, as suggested by ref. 18 (see Fig. 8a). However, when a portable microscope (*Dino-Lite Premier*) is employed to look closely at the channels, the rough, irregular surface of the features

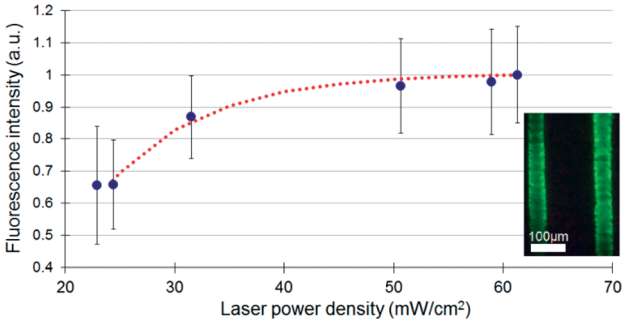

Fig. 7 Normalized fluorescence intensity of etched PDMS as a function of laser power density (inset: fluorescence under 485 nm light of two parallel channels etched at 32 mW cm^{-2} and cleaned with water).

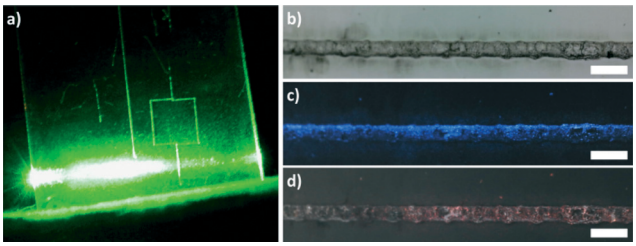

Fig. 8 Waveguide and scattering of etched channels using a green He–Ne laser shone laterally onto the side of the PDMS layer (a). Detail of the central channel seen under a microscope using blue and red laser diodes (c–d). (b) is the reference seen under white light. Scale bars are 200 µm.

seems to promote scattering more than light guiding, although some guiding is still observed (Fig. 8b, c and d). Moreover, when some residues are left inside the channels, light scattering seems to be more prominent.

Conclusions

PDMS laser microfabrication has enabled the development of new applications in photonics, fluidics, bioengineering and complex lab-on-a-chip devices with combinations of these fields. We have demonstrated that microscopic clusters of carbon materials can be used together with a low-cost near-infrared laser to generate micro-plasma at the interface of PDMS layers with air. By understanding this laser-induced incandescence, it was possible to etch superficial microscale volumes of PDMS in a direct, controlled fashion for the rapid-prototyping of integrated microchannels and also to obtain interesting photonics features. The simple platform assembled in this work also offered good control of all the required parameters to fabricate complex micropatterns in PDMS in a CNC fashion. It also allows for modifying the physicochemical properties of PDMS locally, in a similar way to what is typically achieved with expensive high-power lasers. Furthermore, it is evident that the ablation process left combustion residues in the form of carbon nanodomains with interesting properties; in particular, local fluorescence and increased hydrophobicity were readily observed inside the etched volumes.

Acknowledgements

The work has been supported by DGAPA-PAPIIT (grants IN111711 and IN117911), CONACyT (grants 154464 and 153353) and ICyTDF (grant PINV11-17). We would also like to thank: Mario Monroy Escamilla, Jaqueline Cañetas Ortega (SEM); Mariana Cerda Zorilla, Juan Carlos Castro Alcántara (Raman); Tatiana Fiordelisio Coll, Francisco Reyes Mora (fluorescence microscopy) and Brenda Reyes Peraza (CA measurements).

Notes and references

1 J. Cooper McDonald and G. M. Whitesides, *Acc. Chem. Res.*, 2002, **35**(7), 491–499.
2 E. Menard, M. A. Meitl, Y. Sun, J.-U. Park, D. J.-L. Shir, Y.-S. Nam, S. Jeon and J. A. Rogers, *Chem. Rev.*, 2007, **107**(4), 1117–1160.
3 D. A. Chang-Yen, R. K. Eich and B. K. Gale, *J. Lightwave Technol.*, 2005, **23**(6), 2088–2093.
4 S. Thorslund, R. Larsson, F. Nikolajeff, J. Bergquist and J. Sanchez, *Sens. Actuators, B*, 2007, **123**, 847–855.
5 A. Mata, E. J. Kim, C. A. Boehm, A. J. Fleischman, G. F. Muschler and S. Roy, *Biomaterials*, 2009, **30**, 4610–4617.
6 S. M. Azmayesh-Fard, E. Flaim and J. N. McMullin, *J. Micromech. Microeng.*, 2010, **20**, 087002.
7 Y. Xia and G. M. Whitesides, *Annu. Rev. Mater. Sci.*, 1998, **28**, 153–84.
8 D. Qin, Y. Xia and G. M. Whitesides, *Nat. Protoc.*, 2010, **5**(3), 491–502.
9 H. Jin Nam, J.-H. Kim, D.-Y. Jung, J. Bae Park and H. S. Lee, *Appl. Surf. Sci.*, 2008, **254**(16), 5134–5140.
10 B. Schnyder, T. Lippert, R. Kötz, A. Wokaun, V.-M. Graubner and O. Nuyken, *Surf. Sci.*, 2003, **532–535**, 1067–1071.
11 D. Bodas and C. Khan-Malek, *Sens. Actuators, B*, 2007, **123**, 368–373.
12 K. Haubert, T. Drier and D. Beebe, *Lab Chip*, 2006, **6**, 1548–1549.
13 I. Wong and C.-M. Ho, *Microfluid. Nanofluid.*, 2009, **7**, 291–306.
14 J. Zhou, A. V. Ellis and N. H. Voelcker, *Electrophoresis*, 2010, **31**, 2–16.
15 L. W. Luo, C. Y. Teo, W. L. Ong, K. C. Tang, L. F. Cheow and L. Yobas, *J. Micromech. Microeng.*, 2007, **17**, N107–N111.
16 P. Holgerson, D. S. Sutherland, B. Kasemo and D. Chakarov, *Appl. Phys. A: Mater. Sci. Process.*, 2005, **81**(1), 51–56.
17 F. Dausinger, H. Hugel and V. I. Konov, *Proceedings of SPIE 5147, ALT'02 International Conference on Advanced Laser Technologies*, 2003, p. 106.
18 K. L. N. Deepak, S. Venugopal Rao and D. Narayana Rao, *Opt. Eng.*, 2012, **51**(7), 073402.
19 T. N. Kim, K. Campbell, A. Groisman, D. Kleinfeld and C. B. Schaffee, *Appl. Phys. Lett.*, 2005, **86**, 201106.
20 H. Selvaraj, B. Tan and K. Venkatakrishnan, *J. Micromech. Microeng.*, 2011, **21**, 075018.
21 M. Jin, X. Feng, J. Xi, J. Zhai, K. Cho, L. Feng and L. Jiang, *Macromol. Rapid Commun.*, 2005, **26**(22), 1805–1809.
22 C. Dupas-Bruzek, O. Robbe, A. Addad, S. Turrell and D. Derozier, *Appl. Surf. Sci.*, 2009, **255**, 8715–8721.
23 M. Hautefeuille, A. K. Jimenez-Zenteno, P. Perez-Alcazar, K. Hess-Frieling, G. Fernandez-Sanchez, V. Velazquez, M. Grether-Gonzalez and E. Lopez-Moreno, *Appl. Opt.*, 2012, **51**(8), 1171–1177.
24 Z. H. Lim, A. Lee, Y. Zhu, K.-Y. Lim and C. H. Sow, *Appl. Phys. Lett.*, 2009, **94**, 073106.
25 Z. H. Lim, A. Lee, K.-Y. Lim, Y. Zhu and C. H. Sow, *J. Appl. Phys.*, 2010, **107**, 064319.
26 M. Hautefeuille, V. Velazquez, J. Hernández-Cordero, R. Pimentel, L. Cabriales, E. López-Moreno and M. Grether, "Laser Direct Microfabrication Using Light-Induced Nanoparticle Incandescence," in *Advanced Photonics Congress, OSA Technical Digest (online)*, Optical Society of America, 2012, paper ITu4C.5.
27 M. T. Khorasani, H. Mirzadeh and Z. Kermani, *Appl. Surf. Sci.*, 2005, **242**(3–4), 339–345.
28 K. L. N. Deepak, R. Kuladeep, S. Venugopal Rao and D. Narayana Rao, *Chem. Phys. Lett.*, 2011, **503**, 57–60.
29 W. Yang, P. G. Kazansky and Y. P. Svirko, *Nat. Photonics*, 2008, **2**, 99–104.
30 J. Cordelair and P. Greil, *J. Eur. Ceram. Soc.*, 2000, **20**, 1947.
31 T. Luo, K. Esfarjani, J. Shiomi, A. Henry and G. Chen, *J. Appl. Phys.*, 2011, **109**, 074321.
32 W. Huang, W. Qian and M. A. El-Sayed, *J. Am. Chem. Soc.*, 2006, **128**, 13330–13331.
33 R. Pimentel-Dominguez, F. M. Sanchez-Arevalo, M. Hautefeuille and J. Hernández-Cordero, *Smart Mater. Struct.*, 2013, **22**, 037001.
34 D. A. Cremers and L. J. Radziemski, *Handbook of Laser-Induced Breakdown Spectroscopy*, Wiley, New York, 2006.
35 National Institute of Standards and Technology, http://www.nist.gov/pml/data/asd.cfm.
36 A. Genovese and R. A. Shanks, *Composites, Part A*, 2008, **39**, 398–405.
37 V.-M. Graubner, A. Wokaun, O. Nuyken, S. Lazare, T. Lippert and L. Servant, *Appl. Surf. Sci.*, 2006, **252**, 4781–4785.
38 G. Camino, S. M. Lomakin and M. Lageard, *Polymer*, 2002, **43**(6), 2011–2015.
39 A. Saha, R. Raj and D. L. Williamson, *J. Am. Chem. Soc.*, 2006, **89**(7), 2188–2195.
40 S. Kopetz, D. Cai, E. Rade and A. Neyer, *AEU Int. J. Electron. Commun.*, 2007, **61**(3), 163–167.
41 A. Usman Zillohu, R. Abdelaziz, M. Keshavarz Hedayati, T. Emmler, S. Homaeigohar and M. Elbahri, *J. Phys. Chem. C*, 2012, **116**(32), 17204–17209.
42 J. P. Lewicki, J. J. Liggat and M. Patel, *Polym. Degrad. Stab.*, 2009, **94**, 1548–1557.

